2012 IEEE International Conference on Power Electronics, Drives and Energy Systems
December16-19, 2012, Bengaluru, India

A Novel Three-Phase Bi-directional, Isolated, Single-Stage, DAB-based AC-DC converter with Open-loop Power Factor Correction

Gysler Castelino
University of Minnesota
Email: caste034@umn.edu

Kaushik Basu
University of Minnesota
Email: basux017@umn.edu

Ned Mohan
University of Minnesota
Email: mohan@umn.edu

***Abstract*—In this paper, a modulation method for a single-stage three-phase AC-DC converter with only two active switches on the AC-side is proposed. The Dual Active Bridge (DAB) based modulation provides the advantages of Zero Current Switching (ZCS) for the primary side switches, linear power relationship for easy control implementation and unity power factor with open-loop control. Some other features of this topology are galvanic isolation and bi-directional power flow capability. This converter is analysed and the conclusions of the analysis and simulation concur.**

I. Introduction

Three-phase AC-DC conversion was traditionally achieved using thyristor converters and diode-bridge rectifiers, however due to power quality issues, various other power electronic topologies were explored [1]. Transformer isolation is essential in some applications like UPS in order to provide separate grounding for critical loads, prevent leakage currents and safety [2]. Using a high-frequency transformer (HFT) instead of a line-frequency transformer results in reduced converter size and weight and consequently increased power density. A number of three-phase AC-DC converters have been proposed that employ HFT instead of line frequency transformers. HFT isolated AC-DC converters can be classified into multi-stage converters and single-stage converters.

In multi-stage HFT isolated AC-DC converters, typically, the input current and power factor control is achieved in the first stage involving AC-DC conversion and the following stage is a DC-DC converter that is used to regulate the DC voltage. The two-stage converters proposed in [3], [4] (three-phase) and [5], [6] (single-phase) have bi-directional power flow capabilities making them suitable for motor drive application for regenerative braking and battery charging/discharging in electric/ hybrid vehicles. In [5] and [6], [4], the DC-DC converter stage is soft-switched and operates under phase shift modulation (PSM). This PSM or dual active bridge principle (DAB) was first proposed in [7], [8]. Because of their inherent soft-switching characteristics, and consequently low switching losses, these converters can operate at a high switching frequency and further reduce the size of HFT and required filters. These converters use the leakage inductance of the HFT for power transfer. However, the problems with multi-stage conversion are low efficiency and reduced reliability.

Single-stage, HFT isolated, three-phase AC-DC converters with soft-switching (ZVS or ZCS) have been proposed [9], [10], [11]. In [9], [10] the transformer leakage inductance facilitates soft-switching; however, in [11] it must be minimized to reduce losses. All these converters lack bi-directional functionality.

Single-stage bi-directional isolated AC-DC converters that use cycloconverter are proposed in [12], [13], [2] (full-bridge) and [14] (half-bridge). These converters are used for motor drive applications. The drawbacks of these converters are: commutation of the AC-side switches is complex and these converters require four-quadrant switches on the AC-side. In these converters, the transformer leakage inductance needs to be very small for safe commutation of switches. In some cases, snubber circuitry is also necessary. The leakage inductance commutation will limit the switching frequency of the HFT [13]. A topology for Vehicle to Grid (V2G) application is proposed in [15], this topology uses the transformer leakage inductance for power transfer, has ZCS and open loop power factor correction; however, this converter requires 6 four-quadrant switches on the AC side.

In this paper, a three-phase bi-directional, HFT isolated, single-stage, DAB-based, AC-DC converter (shown in Fig. 1) which was proposed in [16] is analysed. This converter has only two active switches on the AC-side. The transformers provide isolation and their leakage inductance is used for power transfer. This topology combines all the advantages of a HFT based system and a DAB-based system. No clamp circuit is required for this converter. In Section II, the topology and modulation technique are introduced. In the following section, the converter is analysed and in the last section, the analytical results are compared with the simulation results.

II. Topology and Modulation Technique

The three-phase AC-DC converter system is shown in Fig. 1. Balanced three-phase AC voltages given by (1) are applied to a bank of three three-winding transformers. The turns-ratio of one half of the primary winding to the secondary winding is $1 : n$. The secondary side of the transformer is connected to a DC voltage source, V_{dc} through a two-level converter. In this topology, $V_{dc} > \sqrt{3}n\hat{V}_i$. All the switches on the DC side are two-quadrant. The AC side switches S_1 and S_2 are

978-1-4673-1508-5/12/$31.00 ©2012 IEEE

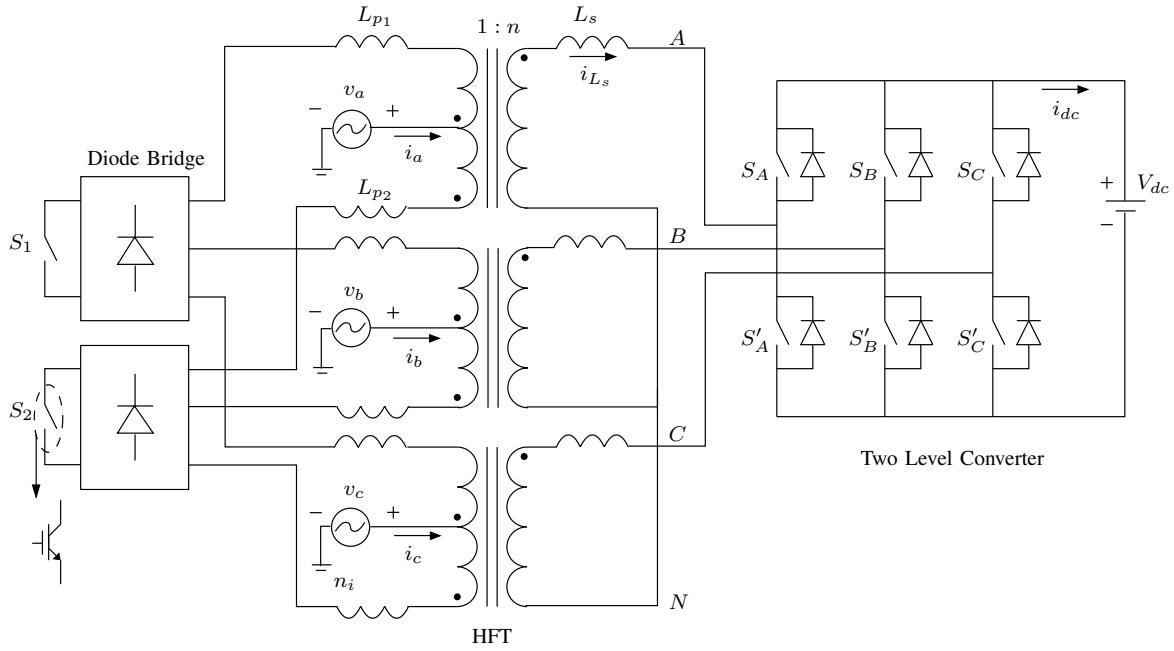

Fig. 1. Three-phase AC-DC converter: Topology

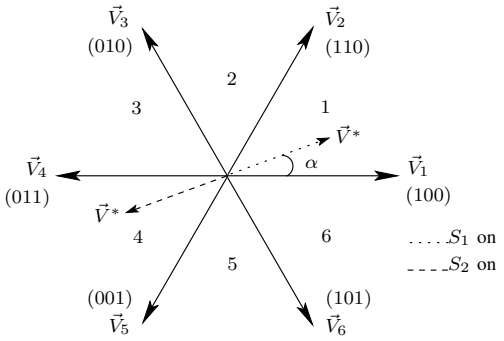

Fig. 2. Switching vectors

realized using a three-phase diode bridge and 1 one-quadrant switch. S_1 and S_2 are switched in a complementary way, with 50% duty at a switching frequency $f_s \left(= \frac{1}{T_s}\right)$ where, $f_s \gg f$. Hence high-frequency AC voltages are applied to the transformer primary. Assuming the leakage inductance of the two primary windings are identical ($L_{p_1} = L_{p_2} = L_p$) and the magnetizing inductance is neglected, the primary side circuit and HFT referred to the secondary side can be represented by three balanced voltages v'_x (where, x denotes a, b or c phase) with equivalent transformer leakage inductances in series with it. v'_x is $+nv_x$ when S_1 is on and $-nv_x$ when S_2 is on. The per-phase equivalent leakage inductance referred to the secondary side is given by $L_{eq} = n^2 L_p + L_s$.

The two-level converter is pulse-width modulated to satisfy the following three conditions. 1) Over every $\frac{T_s}{2}$, the average voltage applied across each transformer equivalent leakage inductance must be zero. 2) The switching voltages generated at the transformer secondary side are phase shifted with respect to the primary side voltages; hence, power is transferred by the Dual Active Bridge principle. 3) In this modulation, the phase shift that can be applied is limited such that at any point, the converter can be viewed to be in 'inner mode' of operation.

In order to satisfy the first criterion, the duty ratios for the two-level converter are calculated using conventional Space Vector Modulation (SVM) [17]. The voltage space-vector diagram for a two-level converter is in Fig. 2. In this example, when S_1 is on, the input voltage space vector, $\vec{V}^*$ given by (2) is in sector 1 and when S_2 is on, it is 180^0 out of phase, in sector 4. The duty ratios for vectors $\vec{V}_1$ and $\vec{V}_2$ are given by d_1 and d_2 respectively in (3). As the effective voltage applied across L_{eq} is zero every $\frac{T_s}{2}$ the phase currents of the transformer go to zero at the transition from S_1 to S_2 and vice-versa. Hence, Zero Current Switching (ZCS) is achieved for these switches.

$$
\begin{aligned}
v_a(t) &= \hat{V}_i \cos(\omega t) \\
v_b(t) &= \hat{V}_i \cos\left(\omega t - \frac{2\pi}{3}\right) \\
v_c(t) &= \hat{V}_i \cos\left(\omega t - \frac{4\pi}{3}\right) \qquad \cdots \text{Where, } \omega = 2\pi f \qquad (1)
\end{aligned}
$$

$$
\vec{V}_i(t) = \vec{V}^*(t) = v'_a(t) + v'_b(t)e^{j\frac{2\pi}{3}} + v'_c(t)e^{j\frac{4\pi}{3}} \qquad (2)
$$

$$
\begin{aligned}
d_1 &= \sqrt{3} d \sin\left(\frac{\pi}{3} - \alpha\right) \\
d_2 &= \sqrt{3} d \sin(\alpha) \quad \cdots \text{Where, } d = \frac{n\hat{V}_i}{V_{dc}} \qquad (3)
\end{aligned}
$$

$$
|\delta| \leq \frac{1}{2}\left(1 - \sqrt{3}d\right) \quad \text{Hence, } d_{max} = \frac{1}{\sqrt{3}} \qquad (4)
$$

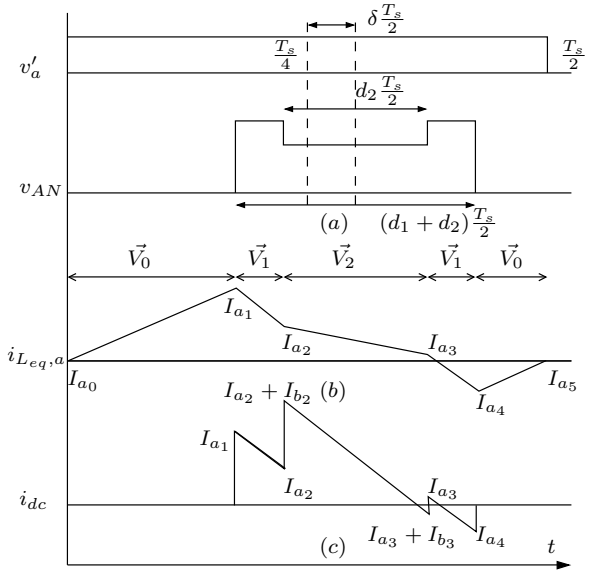

Fig. 3. Switching waveforms

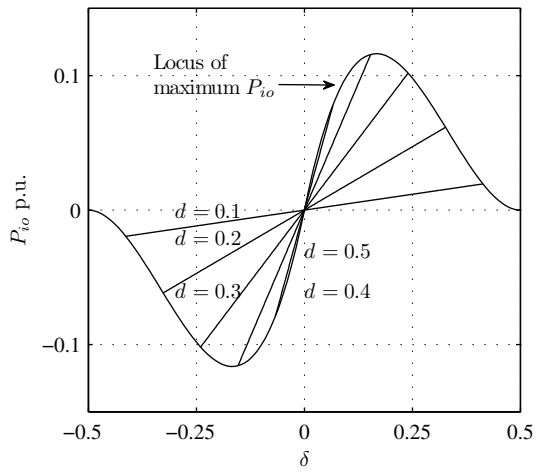

Fig. 4. P_{io} Vs δ

Without loss of generality, the converter waveforms are analysed when $\vec{V}^*$ is in sector 1 and S_1 is on. The secondary side equivalent transformer voltage for phase-a, v'_a and the two-level converter output voltage for phase-a, v_{AN} are shown in Fig. 3(a). A phase shift $\delta\frac{T_s}{2}$ is introduced between the primary and secondary switching voltages of the transformer in order to obtain power transfer and v_{AN} is symmetric with respect to the phase shift $\frac{T_s}{4}+\delta\frac{T_s}{2}$. According to the third condition, the switching pulses for the two-level inverter must be contained within $\frac{T_s}{2}$; thus, δ is limited by (4). When S_1 is on, v_{AN} is 0, $\frac{2}{3}V_{dc}$, $\frac{1}{3}V_{dc}$ when vectors $\vec{V}_0$, $\vec{V}_1$ and $\vec{V}_2$ are applied respectively. The current through L_{eq} for phase-a is shown in Fig. 3(b). As the average value of v_{AN} equals the average value of v'_a over each half cycle, $I_{a_0}=I_{a_5}=0$. This is true for phase-b and phase-c as well. When vector $\vec{V}_0$ is applied, the DC current, i_{dc} (Fig.3 (c)) is zero. When vector $\vec{V}_1$ is applied, $i_{dc}=i_{L_{eq},a}$ and when vector $\vec{V}_2$ is applied, $i_{dc}=i_{L_{eq},a}+i_{L_{eq},b}$.

In order to analyse the currents, voltages and power the per-unit (pu) base values on the secondary side are chosen to be (5). The currents $i_{L_{eq},a}$ and i_{dc} are piecewise linear over the switching cycle; hence, per-unit switching-cycle-average phase currents as well as the DC current of the converter can be calculated to be (6) and (7) respectively. It is clear from (6), if δ is a constant, unity power-factor is obtained on the AC side. The average power per switching cycle, P_{io} is given by (8). The power transferred is directly proportional to δ. The locus of the power that can be transferred for different values of d as a function of δ is plotted in Fig. 4. Maximum power can be transferred (0.1164pu) when d is 0.3849 ($\frac{2}{3\sqrt{3}}$). When δ is positive, power is transferred from the AC side to the DC side, when δ is negative, the power transfer is in the opposite direction.

$$\left.\begin{aligned} V_{base} &= V_{dc} \\ I_{base} &= \frac{V_{dc}}{2\pi f_s L_{eq}} \\ P_{base} &= \frac{V_{dc}^2}{2\pi f_s L_{eq}} \end{aligned}\right\} \tag{5}$$

$$\begin{aligned} \tilde{i_a} &= \pi d\delta\cos(\omega t) \\ \tilde{i_b} &= \pi d\delta\cos(\omega t-\frac{2\pi}{3}) \\ \tilde{i_c} &= \pi d\delta\cos(\omega t-\frac{4\pi}{3}) \end{aligned} \tag{6}$$

$$\tilde{i}_{dc} = 1.5\pi d^2\delta \tag{7}$$

$$\begin{aligned} P_{io} &= \frac{3d^2V_{dc}^2\delta}{4L_{eq}f_s} \\ &= \frac{3d^2\pi\delta}{2}pu \end{aligned} \tag{8}$$

III. Analysis

Every $\frac{T_s}{2}$, the reference voltage space vector, $\vec{V}^*$ is constructed using the two adjacent vectors that make up the sector along with zero vectors. If the zero vector is selected to be 0(000) in all sectors, the vector sequence 0-1-2-1-0 in odd sectors and 0-2-1-2-0 in even sectors will result in minimum number of switch transitions. If 7(111) is selected as the zero vector for all sectors, then switching sequence 7-2-1-2-7 in odd sectors and 7-1-2-1-7 in even sectors will result in minimum number of switch transitions. If the switching sequence is held constant, the zero vector that needs to be applied will change depending on the sector. This will lead to a switching from (111) to (000) every $\frac{T_s}{2}$ because, at that instant, the input voltage reference always switches from an odd sector to even sector or vice-versa.

Since $f_s >> f$, in one switching interval, the input AC-voltages can be assumed to be constant, thus the slope of the

currents in Fig. 3(b), (c) will be linear. The RMS value for the piece-wise linear DC current calculated over $\frac{T_s}{2}$ is denoted by $\overline{I}_{Ts/2}$, it is a function of voltages, d, α and δ. The value of $\overline{I}_{Ts/2}$ is calculated in all 6 sectors for switching sequence 0-1-2-1-0 and 0-2-1-2-0. The RMS current over a sector j, $\overline{I}_j$ is calculated by (9). It can be shown that it is sufficient to calculate the value of $\overline{I}_j$ in sector 1 and 2 only. Further, the RMS value over the low frequency fundamental is calculated by (10). A similar analysis is done for the transformer currents. The choice of switching sequence does not affect the RMS values for the currents and they all result in unity-power factor on the AC-side.

$$\overline{I}_j = \sqrt{\frac{3}{\pi}\int_0^{\frac{\pi}{3}} \overline{I}_{Ts/2}^2 \,\mathrm{d}\alpha} \qquad j \in \{1, 2..6\} \tag{9}$$

$$\overline{I}_{1/f} = \sqrt{\frac{1}{6}\sum_{j=1}^{6} \overline{I}_j^2} \tag{10}$$

The RMS value of the DC-current $\overline{I}_{dc}$ of this converter in per-unit is given by (11). The size of the DC-capacitor is a function of the RMS ripple current content of i_{dc}. This RMS ripple current in the DC capacitor, $\overline{I}_{rpl}$ is calculated by subtracting the DC component from $\overline{I}_{dc}$. The values of $\overline{I}_{rpl}$ given by (12) are plotted for different values of d as a function of δ in Fig. 5. For a certain value of d, the ripple content in the DC capacitor increases as the absolute value of phase shift, $|\delta|$ increases. The maximum value of $\overline{I}_{rpl}$ is 0.137pu when $d = 0.322$.

$$\begin{aligned}\overline{I}_{dc} &= K_2[(\sqrt{3}\left(9d(-45+358d)+40\left(29+360\delta^2\right)\right) \\ &\quad -1890d\pi)\pi d^3]^{\frac{1}{2}} \qquad \text{Where, } K_2 = 0.013 \end{aligned} \tag{11}$$

$$\begin{aligned}\overline{I}_{rpl} &= K_2[(\sqrt{3}(9d(-45+358d)+40(29+360\delta^2)) \\ &\quad -270d(7+48\delta^2)\pi)\pi d^3]^{\frac{1}{2}} \end{aligned} \tag{12}$$

$$\begin{aligned}\overline{I}_{L_{eq}} &= K_1[(-560\sqrt{3}d+27d^2(3\sqrt{3}+8\pi) \\ &\quad +96(\pi+12\delta^2\pi))\pi d^2]^{\frac{1}{2}} \qquad \text{Where, } K_1 = 0.021 \end{aligned} \tag{13}$$

$$\overline{V}_p = d/2 \qquad \overline{V}_s = \sqrt{\frac{2d}{\sqrt{3}\pi}} \tag{14}$$

$$\overline{I}_{L_p} = \frac{\overline{I}_{L_s}}{\sqrt{2}} \qquad \overline{I}_{L_s} = \overline{I}_{L_{eq}} \tag{15}$$

$$\begin{aligned}P_t &= \frac{3}{2}\left[2\overline{V}_p\overline{I}_{L_p} + \overline{V}_s\overline{I}_{L_s}\right] \\ &= \frac{3}{2}\left(\frac{d}{\sqrt{2}} + \sqrt{\frac{2d}{\sqrt{3}\pi}}\right)\overline{I}_{L_s} \end{aligned} \tag{16}$$

The size of the high frequency transformer is related to its VA rating which is given by P_t in (16). Hence, it is important to determine the RMS voltages and currents applied to the high frequency transformer. The RMS value of $i_{L_{eq}}$ in per-unit as a function of d and δ is given by (13). The voltages generated by the two-level converter are applied at the secondary side of the HFT. Since the switching duty ratios as well as the DC voltage is known, the RMS voltages applied to the secondary side of the transformer, $\overline{V}_s$ can be calculated in the same way as the RMS analysis for the currents. The transformer primary and secondary winding RMS voltages $\overline{V}_p$ and $\overline{V}_s$ are given by (14). As each primary winding conducts only for 50% of the time, $\overline{I}_{L_p}$ is given by (15). P_t is plotted as a function of P_{io} for different values of d in Fig. 6. The transformer utilization factor (TUF) is defined as $\frac{P_{io}}{P_t}$. The highest value of TUF 68.8% is obtained for a power transfer of 0.116pu with $d = 0.399$. One drawback of this converter is that, when δ equals zero, the power transfer is zero, however there are RMS currents in the transformer. The worst case occurs when $d = 0.577$ and $P_t = 0.106$pu.

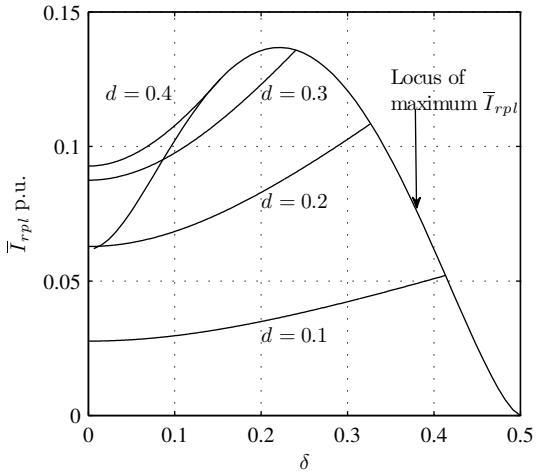

Fig. 5. $\overline{I}_{rpl}$ Vs δ

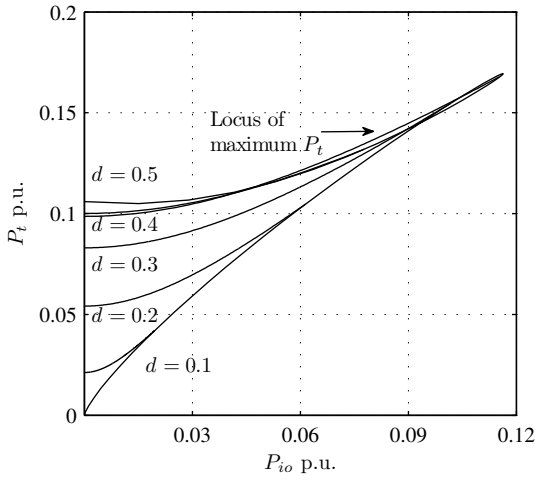

Fig. 6. P_t Vs P_{io}

TABLE I
SIMULATION PARAMETERS

$\hat{V}_i$	120V
V_{dc}	400V
f_s ,f	5kHz , 60Hz
$L_{p_1} = L_{p_2} = L_s$	50μH
$1:n$	1:1

TABLE II
ANALYTICAL AND SIMULATED VALUES

	Analytical	Simulation(δ=0.2)	(δ=-0.2)
$\overline{I}_x$ (A)	21.35	20.98	21.54
$\overline{I}_{dc}$ (A)	19.03	18.55	19.38
$\tilde{i}_{dc}$ (A)	$\pm$10.8	10.31	-11.05
$\overline{I}_{rpl}$ (A)	15.67	14.42	15.87

IV. SIMULATION RESULTS

The converter in Fig. 1 is simulated in Saber. The simulation parameters are listed in Table I. The RMS values for transformer currents as well as DC current are measured for $\delta = \pm 0.2$, these values are compared with their analytical formulas in Table II. There is a slight discrepancy in the values of currents based on the direction of power flow because of losses in the circuit. It has been shown that bi-directional power flow is possible by changing the direction of phase shift. For $\delta = 0.2$, the input current for phase-a (i_a) and the DC current (i_{dc}) are plotted in Fig. 7. The input voltage and filtered current for phase-a are in phase with each other in Fig. 7. Hence, unity power factor can be obtained when δ is constant over one low frequency fundamental. The Fourier spectrum of the input current i_a and i_{dc} are in Fig.8. Both these currents have harmonics at 10kHz ($2f_s$). These high frequency harmonics on the AC side can be easily filtered out using an LC filter with resistive damping across the inductor (L=0.7mH, C=100uF, R=100ohm). The switching pulses for switch S_1, the currents through the AC-side switches and the DC current are shown for one switching cycle in Fig.9. It is clear that the switches S_1 and S_2 are switched at zero current.

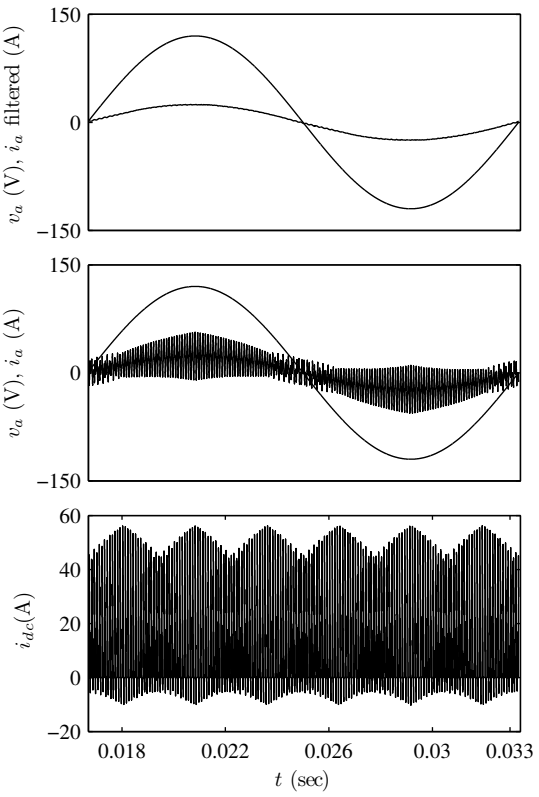

Fig. 7. Simulation results: v_a, i_a filtered, v_a, i_a, and i_{dc}

V. CONCLUSION

A single-stage three-phase AC-DC topology with only two active switches on the AC-side has been analysed in detail. This topology has all the benefits of a high-frequency-transformer system:- voltage transformation ratio, isolation along with high power density. The DAB-based control provides all the benefits of DAB-converters:- soft switching, use of the transformer leakage inductance for energy transfer and compact size. The currents in this converter have high ripple percentage, however this ripple content is at $2 \times f_s$; hence, the size of the filters will be small. The high RMS values for the transformer have to be considered against the benefit of soft-switching. Since the switches S_1 and S_2 are ZCS, a clamp circuit is not required for these switches. The proposed modulation technique results in input side power factor correction

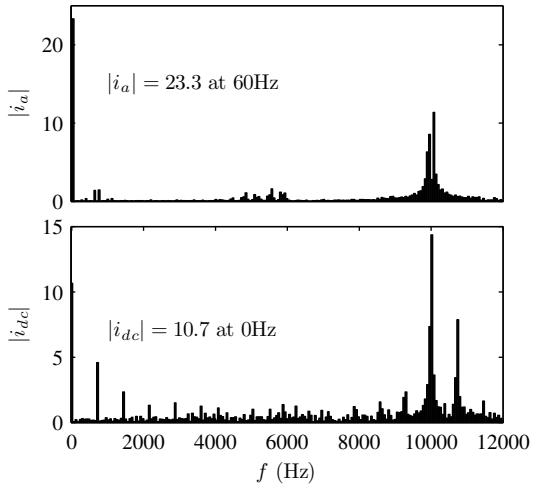

Fig. 8. Simulation results: Fourier spectrum of i_a and i_{dc}

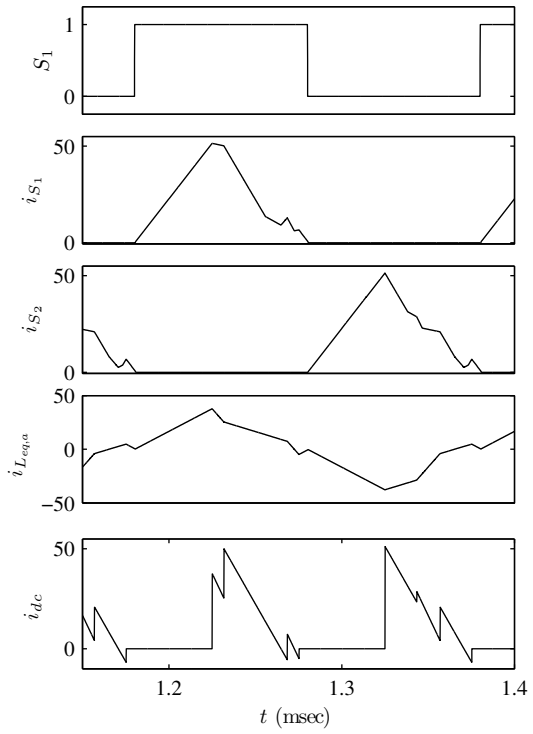

Fig. 9. Simulation results: One switching cycle

under open-loop. The power transfer is directly proportional to the phase shift δ. Hence, the control of this converter is simple.

REFERENCES

[1] B. Singh, B. Singh, A. Chandra, K. Al-Haddad, A. Pandey, and D. Kothari, "A review of three-phase improved power quality ac-dc converters," *Industrial Electronics, IEEE Transactions on*, vol. 51, no. 3, pp. 641 – 660, june 2004.

[2] T. Kawabata, K. Honjo, N. Sashida, K. Sanada, and M. Koyama, "High frequency link dc/ac converter with pwm cycloconverter," in *Industry Applications Society Annual Meeting, 1990., Conference Record of the 1990 IEEE*, oct. 1990, pp. 1119 –1124 vol.2.

[3] J. Zhao, J. Jiang, and X. Yang, "Ac-dc-dc isolated converter with bidirectional power flow capability," *Power Electronics, IET*, vol. 3, no. 4, pp. 472 –479, july 2010.

[4] M.-S. Huang, P.-Y. Yeh, J.-R. Huang, and C.-H. Liao, "Novel bi-directional ac-dc converter for electrical vehicle battery testing," in *IECON 2011 - 37th Annual Conference on IEEE Industrial Electronics Society*, nov. 2011, pp. 1480 –1485.

[5] D. Segaran, D. Holmes, and B. McGrath, "High-performance bi-directional ac-dc converters for phev with minimised dc bus capacitance," in *IECON 2011 - 37th Annual Conference on IEEE Industrial Electronics Society*, nov. 2011, pp. 3620 –3625.

[6] H. Krishnamurthy and R. Ayyanar, "Building block converter module for universal (ac-dc, dc-ac, dc-dc) fully modular power conversion architecture," in *Power Electronics Specialists Conference, 2007. PESC 2007. IEEE*, june 2007, pp. 483 –489.

[7] R. De Doncker, D. Divan, and M. Kheraluwala, "A three-phase soft-switched high power density dc/dc converter for high power applications," in *Industry Applications Society Annual Meeting, 1988., Conference Record of the 1988 IEEE*, Oct. 1988, pp. 796 –805 vol.1.

[8] M. Kheraluwala, R. Gasgoigne, D. Divan, and E. Bauman, "Performance characterization of a high power dual active bridge dc/dc converter," in *Industry Applications Society Annual Meeting, 1990., Conference Record of the 1990 IEEE*, Oct. 1990, pp. 1267 –1273 vol.2.

[9] D. Wijeratne and G. Moschopoulos, "A simple three-phase single-stage ac-dc zvzcs full bridge converter," in *Energy Conversion Congress and Exposition, 2009. ECCE 2009. IEEE*, sept. 2009, pp. 1220 –1227.

[10] V. Vlatkovic, D. Borojevic, and F. Lee, "A zero-voltage switched, three-phase isolated pwm buck rectifier," *Power Electronics, IEEE Transactions on*, vol. 10, no. 2, pp. 148 –157, mar 1995.

[11] Y. Panov, F. Lee, and J. Cho, "A new three-phase ac-dc zero-voltage-switching isolated converter operating in dcm," in *Industry Applications Conference, 1995. Thirtieth IAS Annual Meeting, IAS '95., Conference Record of the 1995 IEEE*, vol. 3, oct 1995, pp. 2602 –2609 vol.3.

[12] S. Norrga, S. Meier, and S. Ostlund, "A three-phase soft-switched isolated ac/dc converter without auxiliary circuit," *Industry Applications, IEEE Transactions on*, vol. 44, no. 3, pp. 836 –844, may-june 2008.

[13] B. Ozpineci and B. Bose, "Soft-switched performance-enhanced high frequency nonresonant link phase-controlled converter for ac motor drive," in *Industrial Electronics Society, 1998. IECON '98. Proceedings of the 24th Annual Conference of the IEEE*, vol. 2, aug-4 sep 1998, pp. 733 –739 vol.2.

[14] R. Garcia-Gil, J. Espi, E. Sanchis-Kilders, V. Esteve, J. Jordan, and E. Maset, "A dsp-controlled four-quadrant ac-dc matrix converter with high-frequency isolation," in *Applied Power Electronics Conference and Exposition, 2004. APEC '04. Nineteenth Annual IEEE*, vol. 2, 2004, pp. 1194 – 1199 vol.2.

[15] N. Weise, K. Basu, and N. Mohan, "Advanced modulation strategy for a three-phase ac-dc dual active bridge for v2g," in *Vehicle Power and Propulsion Conference (VPPC), 2011 IEEE*, sept. 2011, pp. 1 –6.

[16] R. Gupta, K. Mohapatra, N. Mohan, G. Castelino, K. Basu, and N. Weise, "Soft switching power electronic transformer," *U.S. Patent application number: 20110007534*, January 2011.

[17] D. Holmes and T. Lipo, *Pulse Width Modulation for Power Converters: Principles and Practice*, 3rd ed., 2003, vol. 1.